

Control of Stereoerror Formation with High-Activity “Dual-Side” Zirconocene Catalysts: A Novel Strategy To Design the Properties of Thermoplastic Elastic Polypropenes

Ulf Dietrich,[†] Martijn Hackmann,[†] Bernhard Rieger,^{*,†} Martti Klinga,[‡] and Markku Leskelä[‡]

Contribution from the Department for Materials and Catalysis, University of Ulm, D-89069 Ulm, Germany, and Department for Inorganic Chemistry, University of Helsinki, FIN-00014 Helsinki, Finland

Received September 17, 1998. Revised Manuscript Received March 4, 1999

Abstract: The new C_1 -symmetric complexes *rac*-[1-(9- η^5 -fluorenyl)-2-(2-methylbenz[e]-1- η^5 -indenyl)ethane]zirconium dichloride (**14a**), *rac*-[1-(9- η^5 -fluorenyl)-2-(4,5-cyclohexa-2-methyl-1- η^5 -indenyl)ethane]zirconium dichloride (**14b**), and *rac*-[1-(9- η^5 -fluorenyl)-2-(5,6-cyclopenta-2-methyl-1- η^5 -indenyl)ethane]zirconium dichloride (**15**) were prepared in up to 93% yield. These compounds, activated with methyl aluminoxane, exhibit high active propene polymerization rates which remain constant over hours, even at elevated polymerization temperatures of 50 and 70 °C. The two different coordination sites of these “dual-side” catalysts lead to isotactic polypropenes with variable amounts of stereoerrors, depending on the monomer concentration. The 2-methyl substituent of the indenyl ligands results, at the same time, in significantly increased molecular weights of the polymer products (up to 2.3×10^5 g mol⁻¹), the bulk properties of which can be adjusted from flexible, semicrystalline thermoplastic to excellent thermoplastic elastic.

Introduction

It is well established^{1,2} that C_2 -symmetric *ansa*-zirconocene complexes produce isotactic polypropenes. To a lesser degree, research was directed toward C_1 -symmetric metallocene species. However, those structures proved to be excellent tools for the elucidation of the polymerization mechanism, due to the two different coordination sites available for migratory polyinsertion reactions of olefins. Ewen et al.^{3,4} demonstrated that, by varying the structure of the C_s -symmetric complex [2-(9- η^5 -fluorenyl)-2-(η^5 -cyclopentadienyl)propane]zirconium dichloride (**1a**) to the C_1 -symmetric species [2-(9- η^5 -fluorenyl)-2-(3-methyl- η^5 -cyclopentadienyl)propane]zirconium dichloride (**1b**) and [2-(9- η^5 -fluorenyl)-2-(3-*tert*-butyl- η^5 -cyclopentadienyl)propane]zirconium dichloride (**1c**), the stereochemistry of the polymerization reaction can be converted from the production of syndiotactic polypropene to a hemiisotactic form and even to a highly isotactic material by opening or blocking selective and nonselective sites in successive insertion steps.¹

About the same time, Chien et al. introduced the C_1 -symmetric mono-carbon-bridged complex [1-(η^5 -indenyl)-1-(η^5 -tetramethylcyclopentadienyl)ethane]TiCl₂ that produces thermoplastic elastic polypropenes in homogeneous polymerization

reactions at low to ambient temperatures.⁵ Modification of Chien's system toward dimethylsilane-bridged indenyl-cyclopentadienyl zirconium or hafnium complexes by Collins et al.⁶ afforded an improved activity and higher molecular weights. In analogy to the work of Chien, the elastic properties of these new materials were traced back to blocklike structures composed of isotactic and atactic sequences.⁷

Our initial forays into the design of C_1 -symmetric *ansa*-zirconocene dichlorides hinged on the ethylene-bridged diastereoisomers **2a,b** which contain bulky bridge substituents that stabilize the conformation of the metallacycles. This leads to a relatively high stereoselective δ -forward conformer⁸ (**2a**) and to a nearly nonselective λ -backward conformer (**2b**) in polymerization reactions with propene. The most interesting fact was the observation that catalysts derived from **2a** and from the

(5) Mallin, D. T.; Rausch, M. D.; Lin, Y.-G.; Dong, S.-H.; Chien, J. C. *W. J. Am. Chem. Soc.* **1990**, *112*, 2030. Llinas, G. H.; Dong, S.-H.; Mallin, D. T.; Rausch, M. D.; Lin, Y.-G.; Winter, H. H.; Chien, J. C. *W. J. Am. Chem. Soc.* **1992**, *114*, 1242. Chien, J. C. W.; Llinas, G. H.; Rausch, M. D.; Lin, Y.-G.; Winter, H. H.; Attwood J. L.; Bott, S. G. *J. Am. Chem. Soc.* **1991**, *113*, 8569. Chien, J. C. W.; Llinas, G. H.; Rausch, M. D.; Lin, Y.-G.; Winter, H. H.; Attwood J. L.; Bott, S. G. *J. Polym. Sci., Part A* **1992**, *30*, 2601.

(6) Bravakis, A. M.; Baily, L. E.; Pigeon, M.; Collins, S. *Macromolecules* **1998**, *31*, 1000–1009. Gauthier, W. J.; Corrigan, J. F.; Taylor, N. J.; Collins, S. *Macromolecules* **1995**, *28*, 3771–3778.

(7) Studies of Waymouth et al. on the unbridged bis(2-phenylindenyl)-zirconocene dichloride showed the possibility of producing thermoplastic polypropene elastomers. For references, see, e.g.: (a) Coates, G. W.; Waymouth, R. M. *Science* **1995**, *267*, 217–219. (b) Bruce, M. D.; Coates, G. W.; Hauptmann, E.; Waymouth, R. M.; Ziller, J. W. *J. Am. Chem. Soc.* **1997**, *119*, 11174–11182. (c) Tsvetkova, V. I.; Nedorezova, P. M.; Bravaya, N. M.; Savinov, D. V.; Dubnikova, I. L.; Optov, V. A. *Polym. Sci., Ser. A* **1997**, *39* (3), 235–240 and literature cited there.

(8) The terms “ δ -forward” and “ λ -backward” refer to the conformation of twisted metallacycles; for definitions and closer discussion, cf.: (a) Corey, E. J.; Bailer, J. C., Jr. *J. Am. Chem. Soc.* **1959**, *81*, 2620. (b) Rieger, B.; Jany, G.; Fawzi, R.; Steimann, M. *Organometallics* **1994**, *13*, 647–653.

[†] University of Ulm.

[‡] University of Helsinki. Address correspondence about single-crystal X-ray diffraction analysis to these authors.

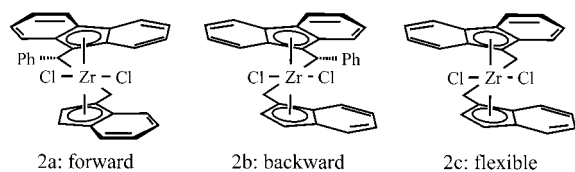
(1) For a recent review, see, e.g.: Brintzinger, H. H.; Fischer, D.; Mühlhaupt, R.; Rieger, B.; Waymouth, R. *Angew. Chem., Int. Ed. Engl.* **1995**, *107*, 1255–1283.

(2) Kaminsky W.; Arndt, M. *Adv. Polym. Sci.* **1997**, *127*, 143–187.

(3) Ewen, J. A.; Jones, R. L.; Razavi, A.; Ferrara, J. D. *J. Am. Chem. Soc.* **1988**, *110*, 6255.

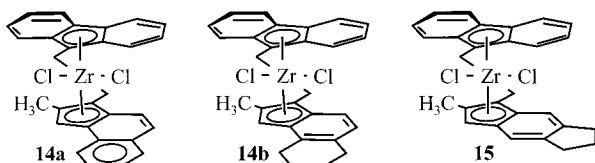
(4) Ewen, J. A.; Elder, M. J.; Jones, R. L.; Haspelslagh, L.; Attwood J. L.; Bott, S. G.; Robinson, K. *Makromol. Chem., Macromol. Symp.* **1991**, *48/49*, 253.

unsubstituted derivative **2c** show a strong decline of the stereoselectivity with the increase in propene concentration, whereas **2b** is nearly independent of monomer concentration.^{8b}



According to theoretical investigations of Guerra and co-workers,⁹ this phenomenon could be attributed to energy differences (2–3 kcal mol⁻¹) for propene coordination to the less hindered (favored) and the more highly substituted side (nonfavored), depending on the bridge conformation. However, catalysts such as **2a–c**/methyl aluminoxane (MAO) produce only low-molecular-weight polymers with low activity, so that control of the formation of stereoerrors could not be used to tailor the microstructure of polypropenes in such a way that new material properties can be created.

In the present paper, we report on the synthesis and the polymerization behavior of the new, ethylene-bridged C₁-symmetric zirconocene dichlorides **14a,b** and **15**, bearing a 2-methyl substituent on the indenyl moiety. The catalysts



resulting after MAO activation show an unexpected high and constant activity toward the polymerization of propene (about 6 times higher) and lead to significantly increased molecular weight products (up to 8 times) compared to **2a–c**. These “dual-side” complexes combine an isoselective side with one leading predominantly to single stereoerrors within one particular species. The fact that this nonselective side can be exposed to migratory insertion reactions depending on the monomer concentration provides a new tool to control the amount and the distribution of single stereoerrors along an isotactic chain. The resulting polypropenes show a variable crystallinity that allows the material properties to be adjusted from tough thermoplastic to excellent elastic.

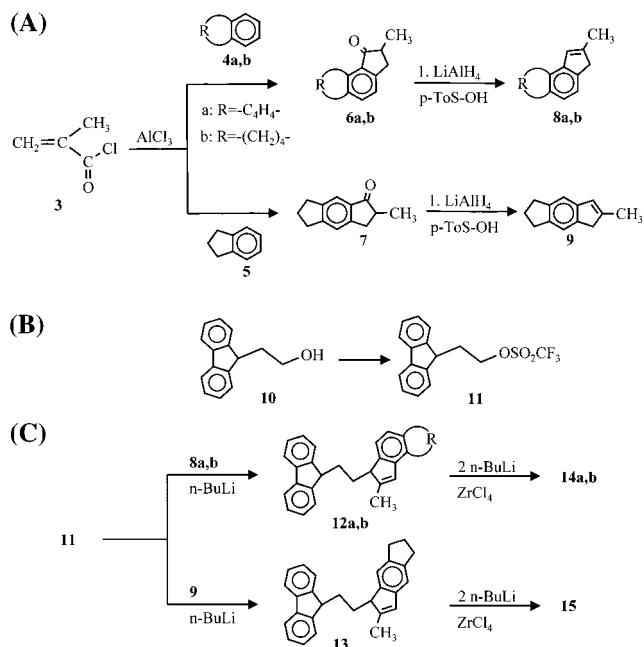
Results

Ligand and Complex Synthesis. A major breakthrough for the synthesis of high-activity C₂-symmetric zirconocene catalysts was the discovery that methyl substitution in the 2-position caused a 3–5-fold increase in the molecular weight,¹⁰ and introduction of a group in the 4-position leads to a significantly increased activity.^{11a,d} The latter substitution pattern is also beneficial to the isotacticity of the polyolefin products. However, the synthetic strategies to suitable indene ligand precursors known so far suffer from either complicated multistep procedures¹¹ or the application of hazardous reactants which limit the tailoring of catalyst leading structures.

(9) Guerra, G.; Cavallo, L.; Moscardi, G.; Vacatello, M.; Corradini, P. *Macromolecules* **1996**, *29*, 4834–4845.

(10) (a) Röhl, W.; Karl, E.; Brintzinger, H. H.; Stehling, U.; Rieger, B. EP 0519237, priority 18.06.1991. (b) Spaleck, W.; Antberg, A.; Rohrmann, J.; Winter, A.; Bachmann, B.; Kiprof, P.; Behm, J.; Herrmann, W. *Angew. Chem., Int. Ed. Engl.* **1992**, *31*, 1347.

Scheme 1



Therefore, we developed a straightforward and highly variable synthetic route toward 2-methylindan-1-ones that lead, in a three-step procedure, to the desired 2-methylindenes in up to 85% overall yield. Starting from methacrylic acid chloride **3**¹² and the readily available substituted benzene derivatives **4a,b** and **5** (Scheme 1A), the indanones **6a,b** and **7** are obtained in a clean reaction. A careful choice of the stoichiometry of the AlCl₃ Lewis acid affords the Friedel–Crafts acylation in all three cases and catalyzes the Nazarov cyclization to give the indanones in up to 96% yield in a one-pot reaction without the need for further purification. This reaction shows a remarkable regioselectivity, too. Whereas the acylation–cyclization sequence leads, in nearly quantitative yields, to the angular benz[*b*]indan-1-one^{11d,13} (**6a**) and tetrahydrobenz[*e*]indan-1-one^{14,15} (**6b**) species, application of the same conditions gives the linear¹⁶ 5,6-cyclopenta-2-methylindan-1-one (**7**) nearly quantitatively. Reduction of **6a,b** and **7** with LiAlH₄ or NaBH₄, followed by

(11) The synthesis of indene leading structures (2,4-substituted indenenes) in clean reactions and high yields is still a challenge. For other approaches, see the following. 4-Phenyl-2-methylindene: (a) Spaleck, W.; Küber, F.; Winter, A.; Rohrmann, J.; Bachmann, B.; Antberg, M.; Dolle, V.; Paulus, E. F. *Organometallics* **1994**, *13*, 954–963. Reaction of γ -diketo derivatives with cyclopentadiene(s): (b) Erker, G.; Nolte, R.; Aulbach, M.; Weiss, A.; Reuschling, D.; Rohrmann, J. DE 41 04 931, priority 18.02.1991. (c) Winter, A.; Antberg, M.; Dolle, V.; Rohrmann, J.; Spaleck, W. EP 0 537 686, priority 15.10.1991. Acylation and cyclization of benzene derivatives with α -bromo isobutyric acid bromide: (d) Stehling, U.; Diebold, J.; Kirsten, R.; Röhl, W.; Brintzinger, H. H.; Jüngling, S.; Mühlhaupt, R.; Langhauser, F. *Organometallics* **1994**, *13*, 964–970. (e) Rohrmann, J.; Küber, F. EP 0 545 304, priority 30.11.1991. Cyclization of benzene derivatives and methacrylic acid with polyphosphoric acid: (f) Kaminsky, W.; Rabe, O.; Schawienold, A.-M.; Schupfner, G. U.; Hanss, J.; Kopf, J. *J. Organomet. Chem.* **1995**, *497*, 181–193.

(12) For the use of methacrylic acid bromide and cycloalkenes in similar reactions, cf.: Hacini, S.; Pardo, R.; Santelli, M. *Tetrahedron Lett.* **1979**, *47*, 4553–4556.

(13) Sülting, C.; Gregorius, H.; Dobler, W.; Hingmann, R.; Rieger, B.; Dietrich, U.; Wagner, J. M.; Müller, H. J. DE 19624828, priority 09.07.1996.

(14) Müller, H. J.; Trübenbach, P.; Rieger, B.; Wagner, J. M.; Dietrich, U. DE 19634684, priority 12.09.1996.

(15) Tetrahydrobenz[*e*]indene was already published before by Brintzinger's group. However, their route using α -bromoisobutyric acid bromide led to a mixture of angular and linear products with 55 and 30% yields, respectively; cf.: Schneider, N.; Huttenloch, M. E.; Stehling, U.; Kirsten, R.; Schaper, F.; Brintzinger, H. H. *Organometallics* **1997**, *16*, 3413–3420.

(16) The “angular” 4,5-substituted isomer is only formed in traces.

Table 1. Polymerization Results of Catalysts **14a,b**/MAO in Comparison to **2c** and EBI

entry	cat.	amount ^d	T_p^b	$[C_3]^c$	yield ^d	t_p^e	activity ^f	T_g^b	T_m^b	\bar{M}_w^g	\bar{M}_w/\bar{M}_n	Al/Zr	[mmmm] ^h
1	14a	2.5	50	0.4	4.8	52	5.37	-8.4	112.8	19.2	1.84	3400	72.6
2		2.5	50	1.1	9.0	31	6.42	-4.8	115.8	38.8	1.96	3400	74.4
3		2.5	50	1.9	40.0	65	7.81	-4.2	117.3	54.4	1.99	3400	74.7
4	14b	2.5	70	1.1	29.9	53	12.54	-10.6	108.3	32.4	3.04	3400	66.3
5		2.5	30	1.1	6.1	103	1.33	-1.8	118.0	67.1	2.92	3400	71.9
6		6.5	30	2.9	44.2	43	3.27	-8.0	111.6	85.1	2.37	2000	69.1
7		2.0	50	0.4	1.9	53	2.67	nd ⁱ	134.2	15.2	1.83	4300	79.5
8		2.0	50	1.1	6.7	29	6.41	nd	128.9	21.8	1.96	8600	78.0
9		2.0	50	1.9	17.7	39	7.04	-5.8	126.5	43.2	1.82	4300	78.4
10		2.0	70	1.1	14.4	45	8.87	nd	132.6	19.9	1.98	4300	78.6
11		2.0	30	1.1	2.5	62	1.12	-6.4	111.7	47.8	2.03	4300	69.8
12		12.8	30	2.9	58.8	46	2.07	-6.9	79, 126.5	55.6	1.86	2000	53.7
13		2c	11	50	0.4	5.7	25	1.26	nd	nd	nd	nd	2000
14	11		50	0.7	7.1	21	2.66	nd	110	27.8	1.8	2000	63.9
15	11		50	1.8	16.6	22	4.06	nd	nd	nd	nd	2000	42.8
16	11		70	0.7	11.4	17	5.69	nd	104	19.3	1.4	2000	59.3
17	5		50	1.9	35.0	62	3.59	-10.1	79.5	33.2	2.17	2000	39.8
18	11	50	3.4	20.3	27	4.1	nd	nd	nd	nd	2000	37.5	
19	EBI ^j	10	50	1.1	61.8	26	13 200	nd	nd	nd	nd	3000	nd

^a In μmol . ^b In $^\circ\text{C}$. ^c In mol L^{-1} . ^d In g , ± 0.3 g. ^e In min. ^f In 10^3 kg of PP (mol of Zr $[C_3]$ h)⁻¹. ^g In 10^{-3} g mol⁻¹. ^h In %, $\pm 2\%$ of stated value. ⁱ nd = not determined. ^j EBI = *rac*-ethylenebis(indenyl)zirconocene dichloride.

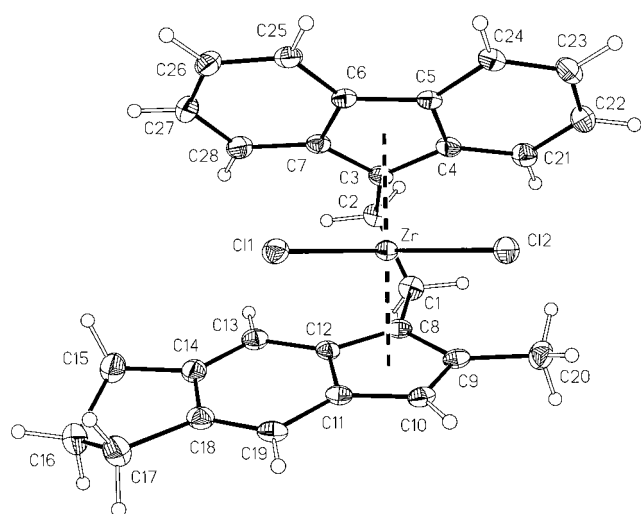


Figure 1. Molecular structure of complex **15** at -100 $^\circ\text{C}$ with 20% probability thermal ellipsoids depicted. Selected distances (\AA) and angles (deg) for complex **15**: Zr(1)–Cl(1), 2.410(2); Zr(1)–Cl(2), 2.430(2); Zr–centroid(Flu) C(3)–C(7), 2.267; Zr–centroid(Ind) C(8)–C(12), 2.226; Cl(1)–Zr(1)–Cl(2), 97.87(6); centroid–Zr–centroid, 128.6.

H_2O elimination, affords the indenenes **8a,b** and **9** as crystalline solids. Ligand and complex syntheses were performed according to our procedure for the formation of ethylene-bridged C_1 -symmetric complexes based on epoxide building blocks (Scheme 1B,C),^{17,18} giving the C_1 -symmetric complexes **14a,b** and **15** in up to 93% yield.

Solid-State Structure. An X-ray structure investigation was performed on the *rac*-[1-(9- η^5 -fluorenyl)-2-(5,6-cyclopenta-2-methyl-1- η^5 -indenyl)ethane]zirconium dichloride (**15**). The bridged structure shows the gross coordination geometry expected for this type of complex.⁸ The sterically demanding ethylene bridge causes a staggered arrangement of both Cp fragments and a δ -backward arrangement of the twisted metallacycle, at least in the solid state (Figure 1). The five-membered cycloalkyl substituent, connected to the ring in the 5,6-position of the

indenyl moiety, shows an envelope form, where the outer CH_2 group points away from the fluorenyl unit. Although the metallacycle of complex **15** was found in a backward arrangement in the solid state, the ethylene bridge is expected to exist in a fast equilibrium between backward and forward isomers in solution.^{8a,17} This hypothesis is supported by variable-temperature ^1H NMR experiments which indicate the existence of only one species between ± 80 $^\circ\text{C}$. For details on single-crystal X-ray-diffraction, see the Supporting Information.

Polymerization Reactions

Activity and Molecular Weight. Among the previously reported C_1 -symmetric precursors **2a–c**, it is the unsubstituted **2c**/MAO which showed the highest polymerization activities (Table 1, entries 13–18). This might be attributed to an increased flexibility of the ethylene-bridged ligand system that allows the complex to adopt an optimal coordination geometry during chain growth. Introduction of the 2-methyl-substituted indenenes **8a,b** and **9** into the ethylene-bridged ligand framework afforded the complexes **14a,b** and **15**, which—after MAO activation—show the highest activity of all C_1 -symmetric propene polymerization catalysts investigated by us to date. In particular, complex **15** (up to 5 times more active than **2c**) gives activities up to 3.2×10^4 kg of PP (mol of Zr mol of C_3 h)⁻¹ at 70 $^\circ\text{C}$ (PP = polypropylene).^{19,20} The polymerization activity increases with the polymerization temperature for all three species. Under identical conditions, the front-substituted benz- and tetrahydrobenzindenyl systems **14a,b**/MAO show the lowest and the side-substituted catalyst **15**/MAO the highest activities.

The 2-methyl substituent of **14a,b** and **15** significantly affects both molecular weight and stereoregularity (Tables 1 and 2) of the resulting polypropenes. A comparison with **2c** (Table 1, entries 13–18) demonstrates that this 2-methyl group leads, for all three complexes, to products with 2–7 times higher molecular weights under comparable conditions. As expected, the molecular weights of the polypropenes can be increased by lowering the polymerization temperature (at constant monomer

(19) This is in the range of Brintzinger's *rac*-Et(Ind)₂ZrCl₂/MAO system tested under similar conditions.

(20) For direct comparison with *rac*-Et(Ind)₂ZrCl₂, entry EBI is given in Table 1; cf. also: Kaminsky, W. *Makromol. Chem. Phys.* **1996**, *197*, 3907–3945.

(17) Rieger, B.; Fawzi, R.; Steimann, M. *Chem. Ber.* **1992**, *125*, 2373–2377.

(18) Rieger, B.; Jany, G.; Steimann, M.; Fawzi, R. *Z. Naturforsch., Part B* **1994**, *49*, 451–458.

Table 2. Polymerization Results of **15**/MAO (Top) and Pentad Distribution of the Polymer Products (Bottom)

entry	amount ^a	T_p^b	$[C_3]^c$	t_p^d	yield ^e	activity ^f	T_g^b	T_m^b	\bar{M}_w^g	\bar{M}_w/\bar{M}_n
20	5.0	50	0.4	46	13.9	8.85	-7.3	101.5	24.1	1.92
21	3.75	50	1.1	72	51.4	10.57	-4.6	95.3	43.0	2.19
22	2.5	50	1.9	50	51.2	13.01	-9.8	96.0	48.0	2.09
23	15	30	1.1	41	31.9	2.88	-11.4	76.1	71.0	1.88
24	2.5	70	1.1	42	60.5	32.02	-10.6	98.6	24.8	2.05
25	10	40	1.1	114	65.6	3.2	-9.8	84.2	48.3	1.95
26	7.5	30	3.9	33	36.9	2.29	-5.9	50.2	171.0	1.96
27	10	35	4.9	39	115.2	3.6	-7.5	51.7	95.7	1.74
28	10	21	4.3	47	53.8	1.61	-4.2	51.0	134.4	1.66
29	15	25	0.7	56	14.6	1.74	nd ⁱ	nd	44.1	1.92
30	15	25	1.6	52	43.2	2.07	nd	nd	63.2	1.88
31	10	30	6.1	25	65.3	2.57	nd	nd	230.0	1.91

entry	[mmmm] ^h	mmmr	rmmr	mmrr	mmrm+rmmr	rmmr	rrrr	rrrm	mrrm	Al/Zr
20	72.1	10.0	no ^j	12.2	2.1	no	no	no	3.6	1700
21	63.9	12.7	0.3	14.2	1.0	0.3	0.3	0.7	6.6	2300
22	59.6	15.9	no	16.5	no	no	no	no	8.0	2300
23	47.8	16.9	1.0	18.6	3.2	0.4	0.8	2.0	9.3	575
24	64.0	14.2	no	12.9	1.2	no	no	0.9	5.8	3400
25	57.1	14.8	0.6	16.3	2.0	0.7	0.5	0.9	7.1	2000
26	36.7	18.5	2.1	21.1	5.0	no	2.5	3.7	10.3	2000
27	36.5	17.9	1.7	21.0	5.8	0.3	3.1	3.6	10.1	2000
28	19.9	17.8	3.2	23.6	9.2	0.4	7.3	8.8	9.8	2000
29	52.9	15.7	0.9	16.9	2.3	0.6	0.8	1.2	8.7	2250
30	37.8	16.9	2.4	19.8	5.2	1.0	2.5	4.1	10.2	2250
31	24.9	17.3	3.1	21.9	8.6	0.2	5.8	7.8	10.4	2000

^a Catalytic, in μmol . ^b In $^\circ\text{C}$. ^c In mol L^{-1} . ^d In min. ^e In g, ± 0.3 g. ^f In 10^3 kg of PP (mol of Zr $[C_3] \text{ h}^{-1}$). ^g \bar{M}_w in 10^{-3} g mol^{-1} . ^h In %, $\pm 2\%$ of stated value. ⁱ nd = not determined. ^j no = not observed.

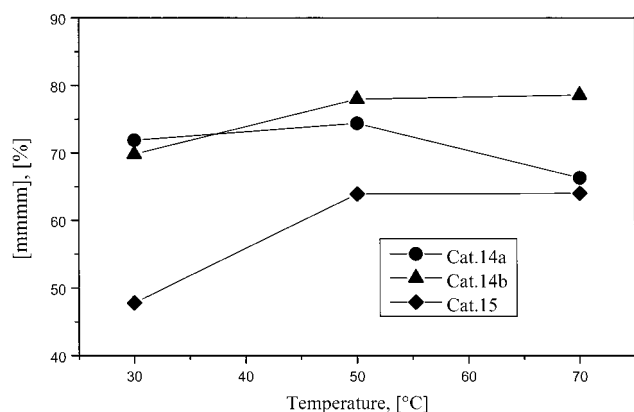


Figure 2. Plot of the propene stereoregularity ([mmmm] pentads) versus the polymerization temperature (T_p) for catalysts **14a,b** and **15**/MAO at constant monomer concentration ($[C_3] = 1.1 \text{ mol L}^{-1}$).

concentration) and by enhancing the monomer concentration (at constant polymerization temperatures). This effect is most pronounced for **15**/MAO, so that a proper combination of both parameters can be used to prepare polymers with molecular weights up to $2.3 \times 10^5 \text{ g mol}^{-1}$ (Table 2, entries 26–29).

Stereoselectivity. All complexes yield isotactic polypropenes with variable amounts of [mmmm] pentads. The three systems **14a,b** and **15**/MAO give polypropenes with [mmmm] concentrations ranging from 53 to 80% (**14a,b**) and from 20 to 72% (**15**), respectively, depending on the indene substituents and the polymerization conditions. Generally, **14a,b**/MAO, which show a front substitution pattern (indene 4,5-substitution, Table 1), give substantially higher isotactic polypropene products than the side-substituted catalyst **15**/MAO (indene 5,6-substitution, Table 2). This behavior can be attributed to the presence of a substituent in the 4-position of the indenyl moiety in **14a,b** compared to **15**. The geometry of **14a,b** is comparable to that of **1c**,²¹ which produces predominantly isotactic polypropenes. The 2-methyl substitution has also a beneficial effect on the

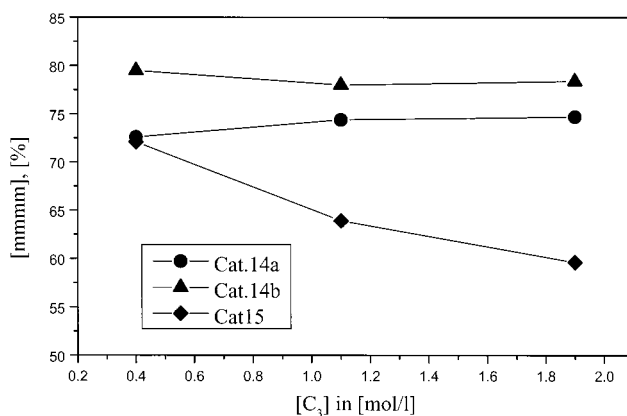


Figure 3. Plot of the propene stereoregularity ([mmmm] pentads) versus monomer concentration ($[C_3]$) for catalysts **14a,b** and **15**/MAO at constant polymerization temperature $T_p = 50 \text{ }^\circ\text{C}$.

stereoselectivity that can be visualized by comparison of **15**/MAO with **2c**/MAO. Under comparable conditions, **15**/MAO produces a polypropene with 60% [mmmm] content, whereas **2c**/MAO gives only 40%. If there is also an effect of the 5,6-cyclopentyl group on the stereoselectivity, it is not yet clear.²²

Interestingly, there is no steady decline of the catalysts' stereoselectivities upon increasing the temperature (Figure 2). The isotacticities of the products prepared with **14b**/MAO at a constant monomer concentration (e.g., 1.1 mol L^{-1}) increase with temperature from 70 (30 $^\circ\text{C}$) to 79% [mmmm] pentads (70 $^\circ\text{C}$). **14a**/MAO gives polypropenes of which the isotacticity goes through a maximum at 50 $^\circ\text{C}$ (74% [mmmm]), and the products of **15**/MAO show an increase of the [mmmm] concentration from 30 (48%) to 50 $^\circ\text{C}$ (64%), after which it remains constant upon a further increase of the polymerization temperature to 70 $^\circ\text{C}$.

(21) Ewen, J. A.; Elder, M. J. EP 537130, priority 07.10.1991.

(22) Cf. also: Lee, I. K.; Gauthier, W. J.; Ball, J. M.; Iyengar, B.; Collins, S. *Organometallics* **1992**, *11*, 2115–2122.

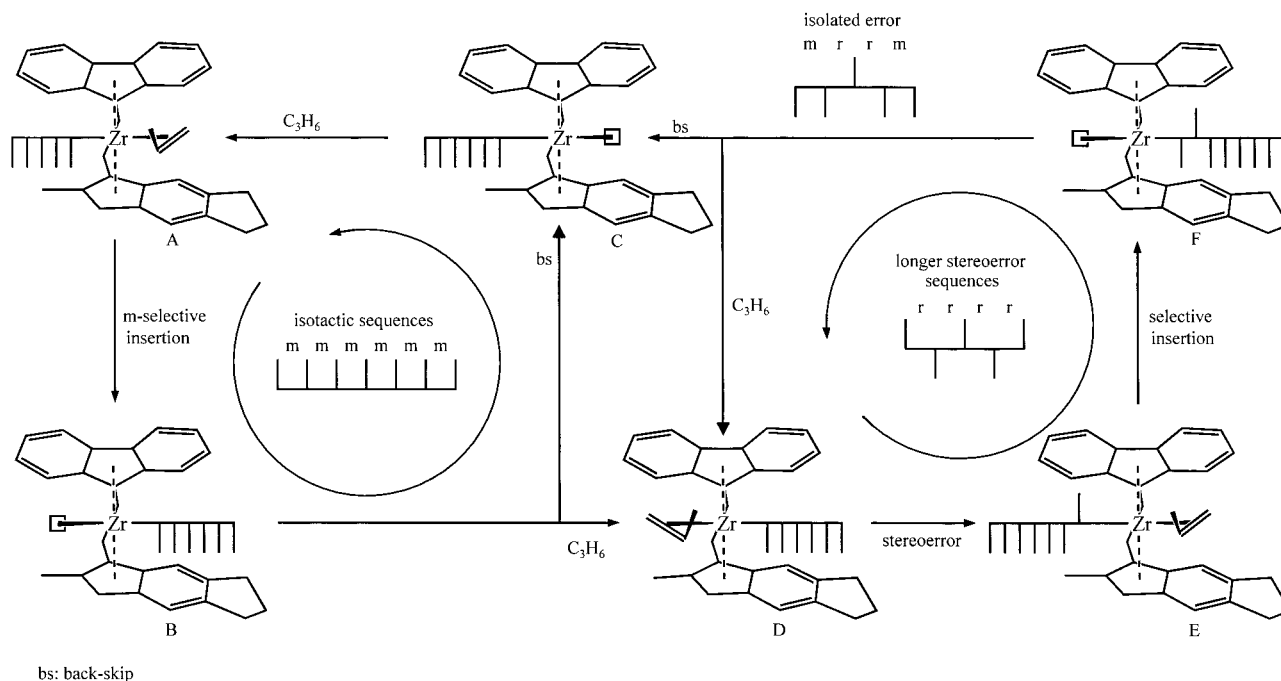


Figure 4. Monomer concentration as a tool for the formation of stereoregularities in high-molecular-weight polypropenes with the “dual-side” system **15**/MAO.

The three catalyst systems differ significantly in the dependence of their stereoselectivity on monomer concentration (Figure 3). Again, the cyclohexasubstituted catalyst **14b**/MAO leads to the highest stereoselectivity which is nearly independent of the $[C_3]$ concentration. The stereoselectivity of the benz[e]-indenyl complex **14a**/MAO increases slightly with the propene concentration. However, the linearly substituted system **15**/MAO shows the highest response on the propene concentration. The isotacticity declines from 72 (0.4 mol L⁻¹) to 60% [mmmm] (1.9 mol L⁻¹). A similar effect was observed by us earlier for **2c**/MAO (Table 1) and for the related phenyl-substituted derivatives **2a,b**/MAO.⁸

Discussion

Stereoselectivity and Monomer Concentration. We attributed the decline of the [mmmm] pentad contents with an increase of monomer concentration to the existence of two coordination sites (Figure 4B,C) in these “dual-side” complexes, which are believed to show different stereoselectivities for monomer coordination and insertion. Guerra et al. supported this hypothesis in an elegant theoretical study,⁹ performed on the complexes **2a,b**. Repeated migratory insertion of the polymer chain to the monomer coordinated between the sterically demanding fluorenyl/indenyl moieties (A → B) and consecutive back-skipping of the growing polymer chain to the free side (B → C) affords isotactic [mmmm] sequences. After each migratory insertion, the chain moves back to the previous position (A) at low monomer concentrations, so that the same coordination site is favored by the chain in successive insertion reactions. The probability of this back-skipping process of the chain is dependent on the difference between the activation energies of the back-skip and the formation of the high-energy alkene-coordinated intermediate (D). Since at low monomer concentrations the back-skipping reaction is faster than monomer coordination, **15**/MAO affords relatively high isotacticities at low $[C_3]$ concentrations and elevated temperatures. An increased $[C_3]$ concentration favors monomer coordination on the less hindered side (D) and leads to the formation of a stereoregular

(D → E). Insertion from E → F proceeds—similar to the process A → B—in a stereoselective way²³ and may lead to the observed rr triad (F).

In the case of **1b**, the insertion from the more to the less hindered side proceeds without a significant enantiofacial discrimination of the prochiral propene molecule. For the polymers obtained with **14a,b** and **15**/MAO, we found that the insertion sequence D → E → F shows a high tendency for the formation of a single rr triad, leading to isotactic polypropenes with variable [mmmm] pentad concentrations. Table 2 summarizes the pentad distributions of some selected materials prepared with **15**/MAO under different conditions. Obviously, higher monomer concentrations lead to a sharp decline of the [mmmm] pentads. At the same time, all the pentads being characteristic for isolated stereoregularities ([mmmr], [mmrr], [mrrm]) increase nearly linearly with monomer concentration (Figure 5). A pentad distribution of [mmmr]:[mmrr]:[mrrm] = 2:2:1 for [mmmm] ≥ 40% indicates also the formation of isolated stereoregularities.

Below 40% [mmmm] pentads, the [mrrr], [rrrr], and [mmrr] signals increase overproportionally, due to the fusion of isolated rr triads to longer error sequences. However, the content of the [rrrr] pentads is not high enough to characterize the polymers as block isotactic–syndiotactic, since the [rrrr] concentration is present in only minor quantities relative to the [mmmm] sequences (Table 2).²⁴

The selectivity for the formation of a single rr triad in the insertion sequence D → E → F (Figure 4) is further supported by the fact that the [mrrm] pentad is absent in the polymer

(23) This insertion process probably proceeds in analogy to C₂-symmetric species after misinsertion; cf.: (a) Corradini, P.; Guerra, G.; Barone, V. *Eur. Polym. J.* **1984**, *20*, 1177–1182 (heterogeneous Ti-based catalytic sites). (b) Cavallo, L.; Guerra, G. *Macromolecules* **1996**, *29*, 2729–2737.

(24) About syndiotactic sequences in polymers formed with backward isomer **2b**, cf. ref 8b. For possible alternative mechanisms of error formation, cf.: (a) Leclerc, M. K.; Brintzinger, H. H. *J. Am. Chem. Soc.* **1995**, *117*, 1651. (b) Song, W.; Yu, Z.; Chien, J. C. W. *J. Organomet. Chem.* **1996**, *512*, 131. (c) Busico, V.; Brita, D.; Caporaso, L.; Cipullo, R.; Vacatello, M. *Macromolecules* **1997**, *30*, 3971.

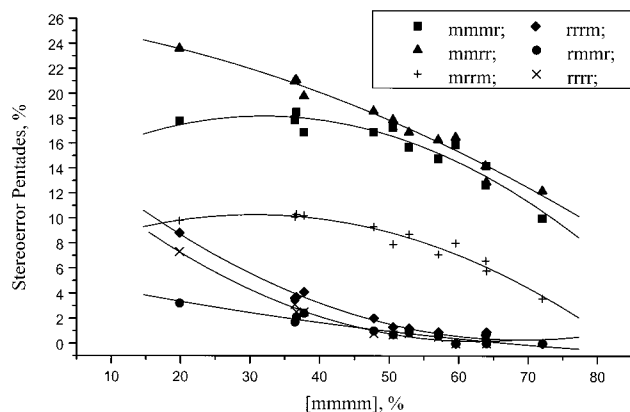


Figure 5. Variation of stereoreerrors (mmmr, mmrr, mrrm, mrrr, rmmr, rrr) in polypropylenes with reduced isotacticity (m[mmmm]) as a fingerprint for the polymerization mechanism.

samples or is detectable in only minor concentrations (Table 2). The same pentad is also not allowed in hemiisotactic polypropylene, due to the occurrence of consecutive selective and nonselective insertions. However, none of our polymer products fits the pentad distribution required for hemiisotactic polypropylene.²⁵ They can be best characterized as isotactic with variable amounts of stereoreerrors.

Based on this approach, the properties of our complexes lie between Ewen's **1b**, which gives hemiisotactic polypropylene by consecutive selective and nonselective insertions, and **1c**, affording highly isotactic materials by blocking the nonselective side. The behavior of **1c** closely resembles that of the front-substituted species **14a,b**. The bulky CH₂ groups of the cycloaliphatic six-membered ring in the activated form of **14b** lead to a fast back-skipping of the chain after a stereoregular insertion happened. The rate of this back-skipping process is accelerated at enhanced temperatures, leading to the observed increase in stereoselectivity (Figure 2) and to the monomer-concentration-independent stereoselectivity (Table 1, entries 7–9). The polymerization behavior of the less sterically hindered front-substituted catalyst system **14a**/MAO supports this hypothesis, since the influence of temperature and monomer concentration is more pronounced and depends on the particular set of parameters applied.

The Design of Material Properties. The linear, 2-methyl-substituted system **15**/MAO gives the highest molecular weight products (up to 2.3×10^5 g mol⁻¹, Table 2, entries 26 and 31) and shows at the same time the best response to the monomer concentration with respect to the formation of stereoreerrors. This allows a fine-tuning of the materials by adjusting the polymerization conditions, so that polypropylenes with properties ranging from crystalline thermoplastic (Figure 6, entries 22 and 25) to thermoplastic elastic (26, 27, and 30) can be achieved. At increased [m[mmmm]] pentad concentrations (higher temperatures, lower [C₃]), the length of the isotactic segments is long enough to afford a higher degree of crystallinity so that these materials display the behavior of tough thermoplastics with relatively high melting temperatures (Table 2, entries 22 and 25). Lower temperatures, together with enhanced propene concentrations, give polymers with molecular weights up to 2.3×10^5 g mol⁻¹, [m[mmmm]] pentad concentration of about 25–40%, and reduced melting temperatures (Table 2 and Figure 6, entries 26, 27, and 30).

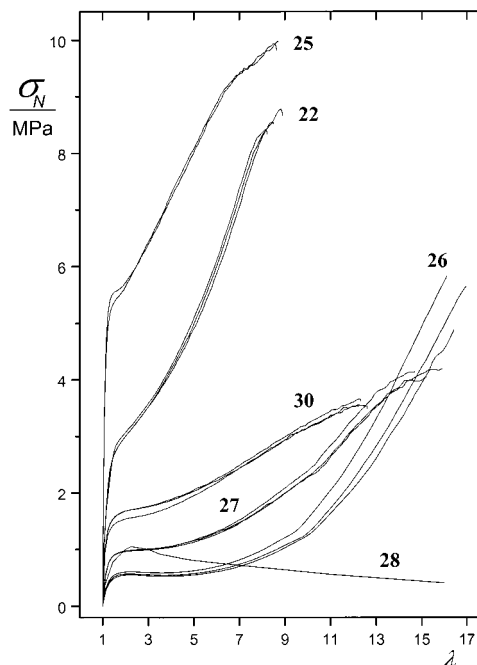


Figure 6. Stress (σ_N)–strain (λ) curves of selected polymers prepared with **15**/MAO: from tough thermoplastics (22, 25) to crystalline elastomers (26, 27, 30) and to viscoelastic polymers (28).

The maximal elongations, λ_B , of these partly crystalline polymers depend on both the isotacticity and the molecular weight of the samples. Reduction of the isotacticity (Table 2, entry 26, [m[mmmm]] = 36.7%) leads to the formation of highly elastic materials with maximal elongations (λ_B) of 17–20 times the original length.²⁶ It is important to point out that these elastic properties cannot be achieved by high-molecular-weight, atactic polymers via chain entanglements. A further reduction of the tacticity (Table 2, entry 28) results in a flexible, highly transparent product, the stress–strain behavior of which (Figure 6, sample 28) shows that the polymer starts to behave like a viscous liquid at higher elongations. Obviously, the interesting elastic property profile results from a reinforcement of the amorphous phase by a crystalline network, which can be tailored by controlling the isotactic block length. The position and length of the elastic plateau of these materials can be tailored together with the initial force to stretch the polymers so that a continuous change of mechanical properties from elastic to thermoplastic can be achieved (Figure 6).

Conclusion

In the present study, we provided a new and highly efficient route toward linear and angular substituted 2-methylindenes. The corresponding C₁-symmetric, ethylene-bridged fluorenyl/indenyl-zirconocene dichlorides are accessible in up to 93% yield without the need for separation of diastereoisomers. This new family of complexes is highly active toward the polymerization of propene after activation with MAO and gives temperature-stable polymerization catalysts. As a new tool, the C₁-symmetry of these “dual-side” catalysts makes it possible to place single stereoreerrors along an isotactic chain, depending on the monomer concentration. The 2-methyl substituent increases, at the same time, the molecular weight of the resulting polypropylenes, so that tacticities of $20 \leq [m[mmmm]] \leq 70\%$ can be combined with molecular weights up to 2.3×10^5 g mol⁻¹.

(25) Farina, M.; Di Silvestro, G.; Sozzani, P. *Macromolecules* **1982**, *15*, 1451. Di Silvestro, G.; Sozzani, P.; Savaré, B.; Farina, M. *Macromolecules* **1985**, *18*, 928–932.

(26) For the first report on the dynamic and viscoelastic properties of the new polymers, cf.: Dietrich, U.; Hackmann, M.; Rieger, B. *Rubber Chem. Technol.* **1998**.

This enables us to tailor the properties of the polymer products from semicrystalline thermoplastic to excellent, nonsticky thermoplastic elastic with high elongations. A preliminary set of scanning force microscopy studies, performed on these elastic polymers in our group, gives a first insight into the size and the distribution of crystallites needed for the formation of a stable three-dimensional network.

In contrast to most of the known catalyst systems for the production of elastic PP, of which structure variations are not possible or lead to nonelastic products, our complexes have a variable structure. It will be interesting to see what kind of material properties of this new family of high-molecular-weight, isotactic poly(1-olefins) with controllable stereoerror sequences will be accessible.

Experimental Section

All reactions were carried out under a dry argon atmosphere using standard Schlenk tube techniques. The hydrocarbon and ether solvents were dried by distillation from LiAlH_4 . CH_2Cl_2 was distilled from CaH_2 and pyridine from NaOH . $(\text{CF}_3\text{SO}_2)_2\text{O}$ ²⁷ and the compounds **10** and **11**⁸ were prepared according to literature procedures. Indane, naphthalene, tetrahydronaphthalene, ZrCl_4 , and AlCl_3 were purchased from Merck and Aldrich, methacrylic acid chloride from Acros, and trifluoromethane sulfonic acid from 3 M Inc. MAO (10% in toluene) was purchased from Witco and toluene for the polymerization reactions from Merck (Licrosolv quality).

Routine ^1H and ^{13}C NMR spectra were recorded on Bruker AC 200 or AMX 500 spectrometers at ambient temperature; chemical shifts are referenced with respect to TMS. Mass spectra were acquired with Finnigan (SSQ 7000) and Varian (MAT-711) instruments. Elemental analyses were determined in the microanalytical laboratory of the University of Ulm.

Polymerization Reactions. The polymerization reactions were performed in a 1-L Büchi steel reactor at constant pressure (± 50 mbar) and temperature (± 0.2 °C). The autoclave was charged with 300 mL of toluene and with the desired amounts of MAO and the zirconocene dichloride. Subsequently, the polymerization temperature was adjusted, followed by charging the reactor with propene up to the desired pressure. The monomer concentrations were measured by the use of a calibrated gas flow meter (Bronkhorst F-111C-HA-33P), and the pressure was kept constant during the entire polymerization period (Bronkhorst pressure controller P-602C-EA-33P). The experimental results were confirmed by comparison with calculated data.²⁸ Pressure, temperature, and the consumption of propene were monitored and recorded online. The polymerization reactions were quenched with acidified MeOH, and the polymer products were precipitated by pouring the toluene solution into excess acidified MeOH. The product was filtered off, washed exhaustively with acidified MeOH and with methanol, and dried in vacuo at 60 °C overnight. The reproducibility of the activity was in the range of $\pm 15\%$, according to several check experiments.

Polymer Analysis. ^{13}C NMR spectra were recorded on a Bruker AMX 500 spectrometer ($\text{C}_2\text{D}_2\text{Cl}_4$, 353 K, with a minimum of 10 000 scans, 2.2 s delay time) and analyzed by known methods.²⁹ According to check experiments, the ^{13}C NMR data sets are correct by $\pm 5\%$ for each peak above 5% of the total area and $\pm 20\%$ below 5%.³⁰ Melting points and glass transition temperatures were measured by differential scanning calorimetry (Perkin-Elmer DSC 7). The data of the second heating run are reported (temperature range -50 – 170 °C, 10 K min^{-1}). Mechanical measurements were performed on a Zwick 1445 tensile apparatus at room temperature with an extension rate of 10 mm min^{-1} .

(27) Beard, C. D.; Baum, K.; Grausskas, V. *J. Org. Chem.* **1973**, *38*, 3673.

(28) For an appropriate equation of state for the system toluene/propene, see, e.g.: Plöcker, U.; Knapp, H.; Pausnitz, J. *Ind. Eng. Chem. Process Des. Rev.* **1978**, *17* (3), 324.

(29) Busico, V.; Cipullo, R.; Corradini, P.; Landriani, L.; Vacatello, M.; Segre, A. L. *Macromolecules* **1995**, *28*, 1887–1892.

(30) For the precision of ^{13}C NMR experiments, see also: Busico, V.; Cipullo, R.; Monaco, G.; Vacatello, M. *Macromolecules* **1997**, *30*, 6251.

All samples were prepared under identical conditions by pressing the polymer melt (170 °C) in vacuo to $10 \times 5 \times 0.1$ -cm specimens, which were cooled to ambient temperature over 20 min. Molecular weights and molecular weight distributions were determined by gel permeation chromatography (GPC, Waters 150 C, 135 °C in 1,2,4-trichlorobenzene) relative to polystyrene and polypropene standards ($\pm 10\%$ of the stated values).

X-ray Crystallography. Crystal data of the compounds were collected with a Rigaku AFC7S single-crystal diffractometer at 193(2) K using $\text{Mo K}\alpha$ radiation (graphite monochromator), $\lambda = 0.71073$ (scan type $\omega/2\theta$). Intensities were corrected for Lorentz and polarization effects. A Ψ -scan absorption correction was performed (TEXSAN)³¹ and solved using SHELXTL/PC.^{32,33} All non-hydrogen atoms were refined anisotropically, hydrogen atoms were placed on calculated positions, and the displacement factors of the H atoms were refined isotropically with full-matrix least-squares techniques to F^2 (SHELXL-93). The final conventional R -value [$I > 2\sigma(I)$] was 0.0324 for complex **15**.

Preparation of 2-Methylbenz[b]indan-1-one (6a), 2-Methyltetrahydrobenz[e]indan-1-one (6b), and 5,6-Cyclopenta-2-methylindan-1-one (7). Naphthalene **4a** (64.03 g, 500 mmol) was added slowly to a suspension of AlCl_3 (134.5 g, 1.01 mol) and methacrylic acid chloride (48.8 mL, 502 mmol) in CH_2Cl_2 (800 mL) at -78 °C. The mixture was subsequently allowed to attain room temperature overnight. The solution was carefully hydrolyzed on ice, and the organic phase was separated. The aqueous phase was extracted twice with CH_2Cl_2 (300 mL), and the combined organic fractions were washed with an aqueous solution of potassium carbonate and dried over sodium sulfate. After removal of the volatile components, **6a** was obtained as a colorless oil (94.39 g, 481 mmol, 96.2%).

The same procedure was used for the preparation of **6b** (**4b**, 30.24 g, 228.7 mmol, gave **6b**, 37.96 g, 189.5 mmol, 82.9%, crystalline solid) and **7** (**5**, 45.84 g, 387.9 mmol, gave **7**, 70.07 g, 376.2 mmol, 97.0%, yellow oil).

Characterization by ^1H NMR, GC–MS, and elemental analysis gave satisfactory values for **6a**^{10a} and **6b**¹⁵ in accordance with literature data.

7: ^1H NMR (200 MHz, CDCl_3) δ 1.25 (d, $J = 6.9$ Hz, 3 H, CH_3), 2.10 (m, $J = 3.7$ – 7.6 Hz, 2 H, CH_2 indan ring), 2.62 (m, 2 H, CH_2 indanone ring system), 2.86 (m, $J = 11$ – 14 Hz, 4 H, CH_2 indan ring), 3.25 (m, $J = 7.0$ Hz, 1 H, CH indanone ring system), 7.21, 7.51 (each s, 2 H, aromatic). MS (GC–MS) m/z 186 (M^+ , 100%). Anal. Calcd: C, 83.83; H, 7.58. Found: C, 83.87; H, 7.54.

Preparation of 2-Methylbenz[e]indene (8a) and 2-Methyltetrahydrobenz[e]indene (8b). **8a**^{10a} and **8b**¹⁵ were prepared according to literature procedures starting from **6a,b**, respectively. LiAlH_4 was used as the reducing agent, and the dehydration was performed in toluene. Chromatographic purification over silica yielded the desired 2-methylindenes **8a,b** as colorless microcrystalline materials. ^1H NMR, GC–MS, and elemental analysis gave satisfactory data in accordance with literature values.

Preparation of 5,6-Cyclopenta-2-methylindene (9). The ketone **7** (70.07 g, 376.2 mmol) was diluted in 500 mL of Et_2O , and the solution was slowly added to a suspension of LiAlH_4 (9 g, 236.8 mmol) in 200 mL of Et_2O . The reaction was stirred for 2 h at ambient temperature and was then carefully treated with water and HCl_{aq} . The organic phase was separated, and the remaining aqueous phase was extracted twice with 300 mL of Et_2O . The combined organic phases were neutralized with K_2CO_3 , washed with water, and dried over Na_2SO_4 . A mixture of the diastereomeric 5,6-cyclopenta-2-methylindan-1-ols was obtained as a crystalline material (69.62 g, 369.8 mmol, 98.3%) after evaporation of the solvent.

This mixture (69.62 g, 369.8 mmol) was dissolved in 600 mL of toluene, and 2 g of *p*-toluene sulfonic acid was added. The solution was heated under reflux using a water separator funnel until no further

(31) Molecular Structure Corp. TEXSAN, Single-Crystal Structure Analysis Software, Version 1.6; MSC: 3200 Research Forest Dr., The Woodlands, TX 77381, 1993.

(32) Sheldrick, G. M. SHELXTL/PC; Siemens Analytical X-ray Instruments Inc.: Madison, WI, 1990.

(33) Sheldrick, G. M. SHELXL-93; University of Göttingen, Germany, 1993.

water was produced (approximately 45 min). The reaction mixture was neutralized by washing with aqueous KOH and was subsequently dried over Na₂SO₄. The toluene solvent was evaporated, and the indene **9** was obtained as a crystalline solid from *n*-pentane (57.67 g, 338.7 mmol, 91.6%).

The indan-1-ols: ¹H NMR (200 MHz, CDCl₃) δ 1.21 (1.13) (d, 3 H, CH₃), 1.76 (broad, 1 H, OH group), 2.05 (m, 2 H, CH₂ indan ring), 2.15–2.71 (m, 2 H, CH₂ indanol system), 2.87 (m, 4 H, CH₂ indan system), 3.08 (m, 1 H, CH₂ indanol system), 4.17 (4.93) (d, 1 H, indanol ring system), 7.07 (7.11), 7.22 (7.28) (each s, 2 H, aromatic). The values in parentheses refer to signals of the minor (approximately 30%) diastereoisomer. MS (GC–MS) *m/z* 188 (M⁺, 100%). Anal. Calcd: C, 82.94; H, 8.57. Found: C, 82.63; H, 8.48.

9: ¹H NMR (200 MHz, CDCl₃) δ 2.23 (m/s, 5 H, CH₂ and CH₃), 3.01 (t, 4 H, CH₂ indan ring system), 3.32 (s, 2 H, CH₂ acidic indene ring), 6.51 (s, 1 H, olefinic indene), 7.20, 7.34 (s, 2 H, aromatic). ¹³C NMR (50 MHz, CDCl₃): δ 16.8 (CH₃), 25.8 (CH₂ indan ring), 32.66, 32.72 (CH₂ indan ring), 42.2 (CH₂ indene system), 127.1 (tertiary C atom indene system), 115.5, 119.5 (aromatic C atoms with H bond), 139.6, 141.7, 142.1, 144.4, 145.0 (aromatic C atoms). MS (GC–MS) *m/z* 170 (M⁺, 100%). Anal. Calcd: C, 91.71; H, 8.29. Found: C, 91.60; H, 8.08.

Preparation of 1-(9-Fluorenyl)-2-(2-methylbenz[e]indanyl)ethane (12a), 1-(9-Fluorenyl)-2-(2-methyltetrahydrobenz[e]indanyl)ethane (12b), and 1-(9-Fluorenyl)-2-(1-(5,6-cyclopenta-2-methylindanyl)-ethane (13). A 6.44-g portion (30.6 mmol) of 2-(9-fluorenyl)ethanol¹⁸ was diluted in 250 mL of CH₂Cl₂, and 2.7 mL of pyridine was added. The solution was cooled to 0 °C, and (CF₃SO₂)₂O (5.3 mL, 9.5 g, 30.6 mmol) was added slowly. The remaining mixture was stirred for 1 h at 0 °C, washed twice with water, and dried over Na₂SO₄. The solvent was removed in vacuo at –10 °C, and the resulting triflate was diluted in 100 mL of dioxane. This solution was added to the lithium salt of **8a**, prepared separately from 4.6 g (25.7 mmol) of **8a** and 16.0 mL of *n*-BuLi in 150 mL of dioxane at 0 °C. The reaction mixture was allowed to attain room temperature overnight and was heated to 60 °C for 30 min. The solvents were evaporated off, and the crude product mixture was dissolved in Et₂O, treated with a saturated aqueous solution of NH₄Cl, and washed twice with water. The separated organic phase was dried over Na₂SO₄, and the solvent was evaporated. Chromatographic purification over silica with a mixture of toluene/hexane (2:3) and crystallization from the same solvent mixture yielded **12a** as a crystalline material (6.85 g, 18.4 mmol, 72.1%).

The same procedure was used for the preparation of **12b** (**8b**, 13.27 g, 72.1 mmol, gave **12b**, 17.47 g, 46.4 mmol, 74.4%, crystalline solid) and **13** (**9**, 3.89 g, 22.85 mmol, gave **13**, 6.49 g, 17.9 mmol, 78.3%, yellow oil).

12a: ¹H NMR (500 MHz, CDCl₃) δ 1.71–1.93 (m, 4 H, CH₂ bridge), 2.49 (s, 3 H, CH₃), 3.25 (s, 2 H, CH benzindene), 4.20 (s, 1 H, CH 9-*H*-fluorene), 7.34–8.13 (m, 14 H, aromatic). MS (FD) *m/z* 372 (M⁺, 100%). Anal. Calcd: C, 93.51; H, 6.49. Found: C, 93.17; H, 6.38.

12b: ¹H NMR (200 MHz, CDCl₃) δ 1.54–1.91 (m, 8 H, CH₂ bridge and six-membered ring), 1.94 (s, 3 H, CH₃), 2.78 (m, 4 H, CH₂ six-membered ring), 3.09 (s, 1 H, indene), 3.88 (t, 1 H, CH 9-*H*-fluorene), 6.52 (m (fine), 1 H, indene olefinic), 6.78–7.83 (m, 10 H, aromatic). MS (FD) *m/z* 376 (M⁺, 100%). Anal. Calcd: C, 92.50; H, 7.50. Found: C, 92.42; H, 7.49.

13: ¹H NMR (200 MHz, CDCl₃) δ 1.41–1.72 (m, 4 H, CH₂ bridge), 1.89 (s, 3 H, CH₃), 2.10 (pseudo-t, 2 H, CH₂ five-membered aliphatic ring), 2.90 (pseudo-t, 4 H, CH₂ five-membered aliphatic ring), 3.06 (s, 1 H, CH indene), 3.87 (t, 1 H, CH 9-*H*-fluorene), 6.40 (s, 1 H, indene

olefinic), 6.98, 7.07 (s, aromatic protons indene system), 7.31–7.77 (m, 8 H, aromatic fluorene). MS (FD) *m/z* 362.5 (M⁺, 100%). Anal. Calcd: C, 92.77; H, 7.23. Found: C, 92.51; H, 6.92.

Preparation of rac-[1-(9-η⁵-Fluorenyl)-2-(2-methylbenz[e]-1-η⁵-indenyl)ethane]zirconium Dichloride (14a), rac-[1-(9-η⁵-Fluorenyl)-2-(2-methyltetrahydrobenz[e]-1-η⁵-indenyl)ethane]zirconium Dichloride (14b), and rac-[1-(9-η⁵-Fluorenyl)-2-(5,6-cyclopenta-2-methyl-1-η⁵-indenyl)ethane]zirconium Dichloride (15). An 857-mg portion (2.3 mmol) of 1-(9-fluorenyl)-2-(2-methylbenz[e]-1*H*-inden-3-yl)ethane (**12a**) was diluted in a mixture of 60 mL of toluene and 5 mL of dioxane and cooled to –78 °C. The ligand precursor was reacted with 2.88 mL of *n*-BuLi at –78 °C, and the reaction mixture was warmed to room temperature over 2 h. Subsequent cooling to –78 °C and addition of solid ZrCl₄ (534 mg, 2.3 mmol) afforded the formation of an orange suspension, which was warmed to room temperature and stirred overnight. The mixture was passed through a 1-in. pad of Celite. The remaining solid fraction was washed with toluene until the organic phase remained colorless. Removal of the solvent gave an orange powder from which the zirconocene dichloride **14a** (447 mg, 0.84 mmol, 36.5%) could be obtained by recrystallization from hot toluene solution.

The same procedure was used for the preparation of **14b** (**12b**, 3.23 g, 8.61 mmol, gave **14b**, 2.73 g, 5.1 mmol, 59.19%, crystalline solid) and **15** (**13**, 1.71 g, 4.72 mmol, gave **15**, 2.30 g, 4.39 mmol, 93.1%, crystalline solid).

14a: ¹H NMR (500 MHz, C₂D₂Cl₄, 80 °C) δ 2.29 (s, 3 H, CH₃), 4.02 (m, *J* = 2–3 Hz, 2 H, CH₂ (fluorene side)), 4.41, 4.93 (m, *J* = 2–3 Hz, each 1 H, CH₂ bridge (indene side)), 6.27 (s, 1 H, indene olefinic), 6.57–8.8 (m, 14 H, aromatic). MS (EI) *m/z* 532 (M⁺, 100%), peak distribution of isotopes according to expected contents. Anal. Calcd: C, 65.72; H, 4.50. Found: C, 65.51; H, 4.12.

14b: ¹H NMR (500 MHz, C₂D₂Cl₄, 80 °C) δ 1.71 (m, 4 H, *J* = 5.9–6.1 Hz, CH₂ cyclohexane ring system), 2.17 (s, 3 H, CH₃), 2.54, 2.65 (each m, 4 H, *J* = 6.1–14 Hz, CH₂ cyclohexane ring system), 4.06 (m, 2 H, *J* = 2.9–9.8 Hz, CH₂ bridge (neighbored fluorene)), 3.82, 4.53 (m, each 1 H, *J* = 2.8–9.7 Hz, CH₂ bridge (diastereotopic)), 6.03 (s, 1 H, indene olefinic), 6.71–7.85 (m, 10 H, aromatic). MS (EI) *m/z* 536, peak distribution of isotopes according to expected contents. Anal. Calcd: C, 64.91; H, 4.88. Found: C, 64.80; H, 4.85.

15: ¹H NMR (500 MHz, C₂D₂Cl₄, 80 °C) δ 2.00 (m, 2 H, *J* = 6.8–7.5 Hz, CH₂ cyclopentane ring), 2.15 (s, 3 H, CH₃), 2.79–2.94 (m, 4 H, *J* = 7.5–9.7 Hz, CH₂ cyclopentane ring), 4.05 (m, 2 H, *J* = 3.5–13.2 Hz, CH₂ bridge (neighbored fluorene)), 3.83, 4.57 (m, each 1 H, *J* = 4.2–10.0 Hz, CH₂ bridge), 6.05 (s, 1 H, indene), 7.03–7.85 (m, 10 H, aromatic). MS (EI) *m/z* 522.6, peak distribution of isotopes according to expected contents. Anal. Calcd: C, 64.35; H, 4.63. Found: C, 64.08; H, 4.63.

Acknowledgment. Generous financial support by the *Deutsche Forschungsgemeinschaft* (SFB 239, F 10), Fonds der Chemischen Industrie, and the *Deutsche Akademische Austauschdienst* DAAD (313/SF-PPP-3/95-kr) is gratefully acknowledged.

Supporting Information Available: Details on single-crystal X-ray diffraction structure analysis of complex **15**, including listings of bond lengths, bond angles, and positional parameters (PDF). This material is available free of charge via the Internet at <http://pubs.acs.org>.